Warren revisited: Atmospheric freshwater fluxes and "Why is no deep water formed in the North Pacific"

Julien Emile-Geay[1]

Département Terre-Atmosphère-Océan, Ecole Normale Supérieure, Paris, France

Mark A. Cane, Naomi Naik, Richard Seager, Amy C. Clement,[2] and Alexander van Geen

Lamont-Doherty Earth Observatory of Columbia University, Palisades, New York, USA

[1]   *Warren*'s [1983] "Why is no deep water formed in the North Pacific" is revisited. His box model of the northern North Pacific is used with updated estimates of oceanic volume transports and boundary freshwater fluxes derived from the most recent data sets, using diverse methods. Estimates of the reliability of the result and its sensitivity to error in the data are given, which show that the uncertainty is dominated by the large observational error in the freshwater fluxes, especially the precipitation rate. Consistent with Warren's conclusions, it is found that the subpolar Atlantic-Pacific salinity contrast is primarily explained by the small circulation exchange between the subpolar and subtropical gyres, and by the local excess of precipitation over evaporation in the northern North Pacific. However, unlike Warren, we attribute the latter excess to atmospheric water vapor transports, in particular the northern moisture flux associated with the Asian Monsoon. Thus the absence of such a large transport over the subpolar North Atlantic may partly explain why it is so salty, and why deep water can form there and not in the North Pacific.   *INDEX TERMS:* 4532 Oceanography: Physical: General circulation; 4283 Oceanography: General: Water masses; 4572 Oceanography: Physical: Upper ocean processes; 1620 Global Change: Climate dynamics (3309); *KEYWORDS:* thermohaline circulation asymmetries, sea-surface salinity, North Pacific Deep Water, monsoons, atmospheric freshwater transports

1. Introduction

[2]   "A notable and well-known asymmetry in the deep circulation is that sinking of surface water to great depth in high northern latitudes occurs only in the North Atlantic, and not at all in the North Pacific" [*Warren*, 1983] (hereinafter referred to as BW). This thermohaline circulation pattern leads, in the Northern Hemisphere, to large differences between the Atlantic and the Pacific oceans, especially concerning the mode of meridional heat transport. *Talley* [1999] estimates that intermediate and deep water formation are associated with at least 75% of the meridional heat transport in the North Atlantic, whereas in the North Pacific it is the shallow gyre overturning that accounts for 75% of this transport. The oceanic meridional heat transport is a significant component of the climate system, and it has been hypothesized in a large number of studies to play a key role in climate change on decadal to millenial timescales, from the onset of the Little Ice Age [*Weyl*, 1968] to glacial-interglacial transitions [*Broecker and Denton*, 1989]. Whether these theories are correct or not, improved understanding of the climate system requires a better knowledge of how the meridional heat transport is determined.

[3]   In attempts to explain this asymmetry, BW posed the central question: "Why is no deep water formed in the North Pacific?" For this problem, the critical variable is the potential density contrast between surface and deep waters. BW related this to the low salinity of the northern North Pacific surface water (32.8‰ on annual mean), "so much lower than the underlying deep water salinities (34.6‰) that even when the surface temperature is reduced to the freezing point,. . . the surface water cannot be made dense enough to sink very deep (wintertime convection seems to be limited to the upper 150 m, as noted by *Reid* [1973])." In contrast, the mean surface salinities of the northern North Atlantic (34.7‰ between 45°N and 60°N) are much closer to the deep water values (34.9‰), allowing for sinking at a sufficiently low surface temperature.

---

[1]Now at Lamont-Doherty Earth Observatory of Columbia University, Palisades, New York, USA.

[2]Now at Rosenstiel School of Marine and Atmospheric Science/MPO, University of Miami, Miami, Florida, USA.
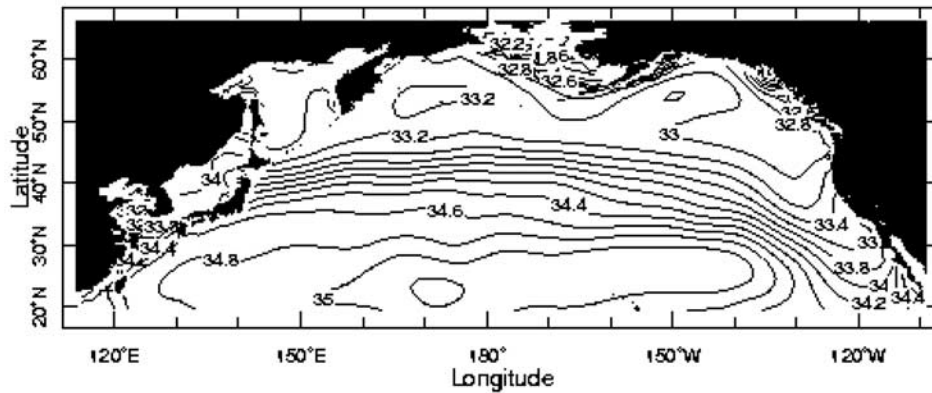
Figure 1. Annual mean salinity (psu) taken from *Levitus and Boyer* [1994] and averaged over the upper 200 m. Note that the isohalines are almost zonal around 40°N, and that the salinity is rather homogeneous north of the main path of the Kuroshio current (roughly 43°N).

[4] Three answers have been offered to BW's question. First, the contrast between the two oceans may be related to the fact that the Atlantic is open to the Arctic whereas the Pacific is largely closed by the Bering Strait and the Aleutians at about 62°N. However, as BW points out, deep water is formed in the Labrador Sea, close to 60°N. In addition, the connection to the Arctic, if anything, would tend to make the North Atlantic fresher. Second, in the North Atlantic, the high salinity of the near-surface layer may be accounted for by the weak freshwater input, due to a much greater evaporation rate than in the North Pacific. This is attributed to the wind-stress curl pattern, which induces northward flow of warm subtropical water in the North Atlantic, whereas in the North Pacific these waters flow largely zonally within the Kuroshio current. Thereby isolated from subtropical water, the northern North Pacific upper layer is eventually freshened by the combined effects of the upwelling, which, while bringing up salty water, also cools the SST and reduces the evaporation, with the latter effect dominating in the salinity budget. This was BW's explanation. Third, the high salinity of the northern North Atlantic upper layer may be more directly due to the high salinity of the Tropical Atlantic, through direct salt advection by the water masses. This salinity is related to atmospheric freshwater fluxes across the Isthmus of Panama [*Weyl*, 1968; *Zaucker et al.*, 1994]. In parallel, the export of water out of the Atlantic basin may be freshening the Tropical Pacific, and consequently the northern North Pacific, through a similar advective mechanism.

[5] A motivation for this study is the growing evidence from paleoceanographic studies that the distribution of several water column properties has fluctuated in the North Pacific on time scales of thousands to hundreds of thousands of years. Such changes have been inferred from sediment cores using proxy records of concentrations of either nutrients [*Boyle*, 1992, and references therein; *van Geen et al.*, 1996; *Keigwin*, 1998] or oxygen [*Dean et al.*, 1989; *Behl and Kennett*, 1996; *Zheng et al.*, 2000] in overlying bottom waters. Various explanations have been proposed to account for these observations, including the possibility of deeper and/or more intense convection at higher latitudes of the North Pacific. Variations in surface

water productivity changes, and their repercussions at depth, provide an alternative mechanism that cannot be ruled out [*Wyrtki*, 1962; *Mix et al.*, 1999]. The notion of climatically sensitive and fairly rapid convection at intermediate depths of the North Pacific has been supported by observations of the penetration of man-made and natural tracers [*Van Scoy and Druffel*, 1993; *Warner et al.*, 1996; *Reid*, 1997] and a time series of hydrographic sections across the basin spanning several decades [*Wong et al.*, 1999]. The objective of this paper is to show with a simple box model that ventilation of the North Pacific is controlled by the transport of water vapor into the region.

[6] The salinity distribution is the result of the balance of oceanic volume transports and boundary freshwater fluxes, i.e., precipitation, evaporation, and continental river runoff. As shown by BW, the simplest way to represent this equilibrium is to consider a steady-state box model in which the freshwater fluxes are balanced by horizontal and vertical advective changes in the salinity of the water passing through the near-surface layer. Here we follow his formulation of the problem, and repeat his calculations with updated estimates of the boundary fluxes involved in the freshwater and salt budgets (section 2). Results and sensitivity analysis are given in section 3 that highlight the importance of moisture convergence over the northern North Pacific. Discussion follows in section 4, and conclusions are given in section 5.

2. A Box Model for the Surface Waters of the Northern North Pacific

2.1. Description

[7] Our study will follow BW and use a box model of the northern North Pacific near-surface layer (hereinafter nNP) to investigate the processes that control its salinity. The box-model formulation is believed to be sufficiently robust for this portion of the ocean since the spatial variability of the salinity field does not exceed 0.5‰. This can be seen in Figure 1. The weak annual variability (less than 0.1‰, using the World Ocean Atlas of *Conkright et al.* [1998]) allows us to consider the system in a steady state for the current equilibrium. On decadal timescales, however, it has
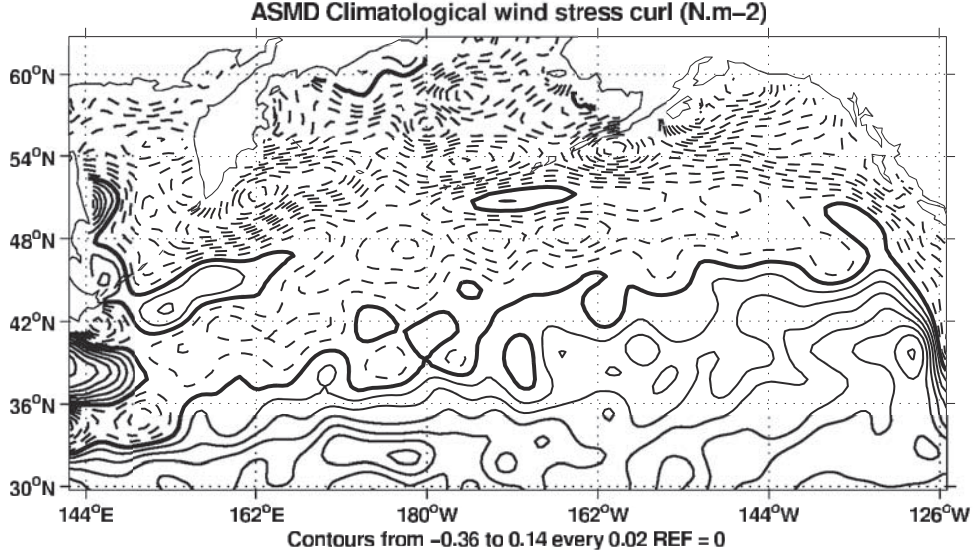
Figure 2. Wind-stress curl over the North Pacific, derived from *da Silva et al.* [1994]. Dashed lines indicate negative curl (Ekman suction), and solid lines indicate positive curl (Ekman pumping). The thick solid line is the zero wind-stress curl line.

been shown to vary significantly: Using hydrological sections along 47°N, *Wong et al.* [1999] inferred a maximum freshening of 0.1‰ in the source region of NPIW over approximately 22 years. As we shall see, this is well below the accuracy permitted by such a crude representation, and will hence be neglected.

[8] The nNP surface layer is taken to be 200 m deep, so that it includes the well-mixed layer in winter. The northern boundary is set at about 60°N by the bathymetry, and the lateral boundaries are the coastlines, between longitudes 143°E and 125°W. The case of the southern boundary is more delicate. To simplify the circulation scheme, BW made this boundary correspond with the zero wind-stress curl line (roughly the boundary between the subtropical and the subpolar gyre), so that the meridional component of the barotropic Sverdrup transport equals zero across this boundary. The wind-stress curl derived from the Atlas of Surface Marine Data is presented in Figure 2. Clearly, the zero wind-stress curl line is not zonal, but if the southern boundary is set at 43°N, the positive and negative areas across the latitude circle may cancel each other. As we shall see later, this is of little importance in our case, for we will estimate the transport across 43°N directly.

[9] Within these boundaries, the average salinity of the nNP box is then $S_s \simeq 33.07‰$, using work of *Levitus and Boyer* [1994], compared with 34.7‰ at 3000 m. In the same latitude domain of the North Atlantic (the northern North Atlantic, hereinafter referred to as nNA), the surface layer salinity is 34.94‰, and about 35‰ at depth.

2.2. Freshwater and Salt Budget for the Surface Waters of the Northern North Pacific

[10] Here we will briefly review BW's formulation, using the same notation. Consider the previously described nNP box of uniform salinity S_s. The boundary fluxes are defined as follows, with the convention that any flux leaving the box is negative:

[11] • The outflow through the Bering Strait V_{BS} carries water of salinity of S_s.

[12] • The Ekman transport occurs across the southern boundary V_E. Since the zonal component of the wind stress is eastward along this line, this flow is southward, hence also transporting water with salinity S_s. However, Sverdrup theory [*Sverdrup*, 1947] requires the following balance in the interior:

$$\beta \int_{-H}^{0} v \, dz = \frac{1}{\rho_0} \hat{k} \cdot \nabla \times \vec{\tau}, \tag{1}$$

where H is the depth of the level of no motion, typically 2000 m. Here $\vec{\tau}$ is the wind-stress vector, and $\hat{k}$ is the local vertical unit vector. This transport vanishes along the zero wind-stress curl line, leading to

$$\int_{-H}^{0} v \, dz = V_E + V_G = 0, \tag{2}$$

where V_E is given by $\frac{\tau_x}{\rho_0 f}$ and $V_G = \int_{-H}^{0} v_G dz$, v_G being the geostrophic meridional velocity. However, while all the Ekman transport occurs in the upper layer, the geostrophic flow is distributed over the whole water column and only a fraction α actually occurs in the upper 200 m (from 0 to $-h$),

$$\int_{-h}^{0} v_G \, dz = \tilde{v}_G = \alpha V_G. $$

[13] BW assumed it to be small, namely $\alpha \sim 1/3$, and we will further show that this estimate lies within an acceptable range of values. Note that the assumption of zero Sverdrup transport (equation (2)) is no longer required here, since we will compute the geostrophic transport independently from the Ekman transport, but the notation will be kept for easier comparison with BW's work. The Sverdrup balance (equation (1)), together with our sign convention, thus yields a

net outflow in the upper 200 m at the southern boundary of $\int_{xw}^{xe}(1-\alpha)V_E\,dx$. However, the relevant quantity for the salt budget is the advective, cross-gyre salt transport M_S. Thus we must not restrict ourselves to a zonally averaged salt transport, for the sign of the integrand at each longitude determines whether subtropical water with salinity S_{WB} (see below) is flowing in, or whether nNP water is being carried out. In contrast with BW, we thus compute the local $V_E + \tilde{v}_G$ as a function of longitude, with even grid spacing. We then group the positive terms in V^+ and the negative terms in V^-, such that the total mass transport is $V = V^+ - V^-$. The meridional, interior salt transport now takes the form

$$M_S = S_{WB}V^+ - S_sV^-, \tag{3}$$

which is a linear function of S_s.

[14] ● The integrated upwelling V_u is produced by the large cyclonic atmospheric circulation, and carrying a salinity S_u.

[15] ● The atmospheric freshwater flux F is the difference between the area-integrated precipitation P, and evaporation E, over the nNP box.

[16] ● The river discharge R flows into the northern North Pacific basin. The total freshwater input is then $R + F$.

[17] ● The "western-boundary current" transport V_{WB} actually groups together the effect of ageostrophic interior flow and nonlinear boundary-layer flow. Its sign is uncertain: Observations of surface currents, especially the Oyashio, suggest a southward, negative V_{WB}, that would carry waters out of the box with salinity S_s. However, as BW argues, there could be an inflow from the subtropical gyre, in this case an extension of the Kuroshio, which "strikes roughly east northeastward after separating from the western boundary farther south and some small part of it may enter the South West portion of the box (V_{WB} northward, positive)." The inflow would then carry water with subtropical salinity S_{WB}. In the model, V_{WB} is calculated as a residual from the mass conservation equation, since it is the most ill-constrained flux.

[18] ● In addition, we now have a better, though largely imperfect, knowledge of the eddy salt fluxes. Using the classical turbulent closure, they can be expressed as the gradients of large-scale quantities. Let us note $\overline{V'S'}$ and $\overline{W'S'}$ the meridional and vertical salt flux and the southern and lower boundaries of the box, respectively. Then,

$$\overline{V'S'} = \iint \kappa_H \left(\frac{\partial S}{\partial y}\right)_{43°N} dx\,dz \tag{4a}$$

$$\overline{W'S'} = \iint \kappa_z \left(\frac{\partial S}{\partial z}\right)_{-200\,m} dx\,dy. \tag{4b}$$

We make the assumption that these do not transport freshwater (in the sense of *Wijffels et al.* [1992]), but only contribute to the salt budget.

[19] The model consists of two conservation equations: (1) mass conservation, where the steady-state assumption together with the continuity equation leads to the following mass balance:

$$R + F + V_u + V_{WB} = V_{BS} + V^+ - V^-, \tag{5}$$

and (2) salt conservation, where the steady-state assumption, together with our parameterization of eddy salt fluxes, reduces the usual advection-diffusion equation to

$$S_uV_u + S_{WB}(V_{WB} + V^+) + \overline{V'S'} + \overline{W'S'} = S_s[V_{BS} + V^-], \tag{6}$$

if V_{WB} is northward, and

$$S_uV_u + S_{WB}V^+ + \overline{V'S'} + \overline{W'S'} = S_s[V_{BS} - V_{WB} + V^-], \tag{7}$$

if V_{WB} is southward.

2.3. Updated Estimates of the Boundary Fluxes

[20] The fluxes were computed from some of the most recent sources, using a $1° \times 1°$ regridding for V_E, F, and V_u. All the data presented here are annual means.

[21] V_{BS}, the outflow through the Bering Strait, is now estimated by *Roach et al.* [1995] to be 0.83 Sv $\pm$ 30% (1 Sv = $10^6/m^3\ s^{-1}$), from moored current meters and direct property measurements over the water column. This result is virtually identical to that of *Coachman and Aagaard* [1981] used by BW (0.8 Sv). Here we have ignored the temporal variations of this transport and simply taken the annual mean, which is northward.

[22] R, the continental runoff, was computed with the Global Runoff Data Center (GRDC) web-based database (available at http://www.grdc.sr.unh.edu) [*Fekece et al.*, 2000]. This raised several problems: (1) Not all the rivers belonging to the Pacific catchment basin are listed in this database, but the contribution of the remaining (smaller) rivers is believed to be negligible. (2) The gauging stations are not always at the mouth of the river, so we took for each one the river discharge time series of the closest station to the ocean; (3) Although the sampling time was not the same for all stations, we performed time averages over the complete time series for each station; this may bias the total river runoff, taken to be the sum of the individual mean river discharges. (4) We made the assumption that all the rivers listed as part of the Pacific catchment basin between 43°N and 60°N were entirely contributing to R, i.e., directly flowing into the nNP box. This might not be the case for the Amur, for example, because the sea of Okhostk is not included in the box we are considering. We find a value of 0.03 Sv, which is likely to be an upper limit, but it might compensate for the problem that not all rivers are accounted for. This error should be small, however, for the five largest rivers (Amur, Yukon, Columbia, Fraser, and Stikine) already account for 87% of this flux. Thus we expect the 11 river flows used in this calculation to capture at least 90% of the real runoff; that is, the error bar should be about 10%. As a comparison, BW used the value of 0.056 Sv, derived from *Baumgartner and Reichel* [1975], which computed the runoff as the residual *P-E* over land, probably a more unreliable approach.

[23] The value of the net atmospheric freshwater flux F is not well-known, due to the large uncertainty in the precipitation fields. The error is reported to be about 30% in this region for the NCEP CPC Merged Analysis of Precipitation (CMAP) [*Xie and Arkin*, 1996], considered as the best product, according to *Trenberth and Guillemot* [1998]. The evaporation rate calculated with the bulk aerodynamic formula is believed to be more accurate, though still subject

Table 1. Atmospheric Freshwater Fluxes Integrated Over the Northern North Pacific (nNP) and Northern North Atlantic (nNA)(Sv)

Data Set	P	E	P-E
	nNP		
GPCP[a]	0.43		
CMAP[b]	0.45		
NCEP[c]	0.40	0.20	0.20
ASMD[d]	0.37	0.16	0.21
P(CMAP)-*E*(ASMD)			0.29
	nNA		
GPCP[a]	0.30		
CMAP[b]	0.35		
NCEP[c]	0.22	0.18	0.04
ASMD[d]	0.27	0.18	0.09
P(CMAP)-*E*(ASMD)			0.17

[a]NASA Global Precipitation Climatology Project (http://precip.gsfc.nasa.gov/).
[b]CPC Merged Analysis of Precipitation [*Xie and Arkin*, 1996].
[c]NCEP-NCAR Reanalyses [*Kalnay et al.*, 1996].
[d]Atlas of Surface Marine Data [*da Silva et al.*, 1994].

to considerable uncertainty. In Table 1 we present results extracted from various data sets.

[24] Integrating the CMAP precipitation field over the box yielded $P = 0.45 \pm 0.15$ Sv. This is the value we will retain for our sensitivity tests. It is noteworthy that the NCEP/NCAR Reanalysis and the *da Silva et al.* [1994] Atlas of Surface Marine Data (ASMD) yield similar, although largely independent, results for the precipitation field. For the integrated evaporation rate we will take $E = 0.18$ *Sv* (compare Table 1), with an error bar of 20%, as done in the ASMD data set [*da Silva et al.*, 1994]. Thus $F = P - E = 0.29 \pm 0.15$ Sv over our box, almost 3 times higher than the *Baumgartner and Reichel* [1975] estimate used by BW (0.095 Sv), but very close to the freshwater divergence calculated by *Roemmich and McCallister* [1989] between 47°N and the Bering strait (0.27 Sv). This introduces a tendency to freshen the nNP relative to BW's calculations.

[25] The Ekman transport through the southern boundary, V_E, was computed using various data sets for the wind stress. Results are presented in Table 2.

[26] The wind stress is also quite uncertain, but no explicit error estimate could be found in the references used here. It is generally admitted to be no larger than 25%. The field belongs to category B in the NCEP/NCAR terminology [*Kalnay et al.*, 1996], which means that its determination involves some model outputs, and should therefore be considered with care. The value given by the TRENBERTH data set is anomalously high, and probably unreliable. Thus we will only consider the first three data sets, and take their arithmetic mean $V_E \sim 5.1$ Sv. BW derived a value of $V_E = 4.5$ Sv from *Fofonoff and Dobson* [1963], which is very similar and only slightly smaller, perhaps because this zonal-integrated quantity was computed over a narrower box.

[27] The interior geostrophic flow V_G can be estimated by a thermal-wind calculation above a reference level (2000 m, as suggested by *Roemmich and McCallister* [1989]), using the density data of *Levitus and Boyer* [1994]. We must note, however, that surprisingly swift currents have been found below that depth in the northwest corner of the basin [*Owens and Warren*, 2001], and that the very existence of a level of no motion should be considered with caution. As

shown by equation (3), the relevant quantity for the salt transport estimate is the sum of the Ekman and geostrophic flow at each longitude, which we computed over boxes of $\Delta\lambda \times \Delta z = 2° \times 200$ m. By consistency, we can verify that the total geostrophic transport between 150.5°E and 125.5°W leads, for this grid spacing, to $V_G = 4.94$ Sv (using a linear interpolation between 42.5°N and 43.5°N). This result is virtually identical to our estimate of V_E (5.1 Sv) at 43°N; thus the assumption of Sverdrup balance across this latitude is not unrealistic, which Figure 2 did not suggest.

[28] The ratio of shallow to total geostrophic transport (0–200 compared to 0–2000), α, is about 0.53, larger than BW's preferred value of 1/3. In Figure 3 we present the Ekman and geostrophic transports as well as the estimated net transport. Integrating along the latitude circle, the total northward transport is $V^+ = 2.02$ Sv, while the southward transport is $V^- = 3.45$ Sv. The net transport is −1.43 Sv. We assume an error bar of 30%, to account for errors is the density field, wind-stress and computational procedure.

[29] For the integrated upwelling V_u, different strategies are available. BW used the upward velocity at the base of the Ekman layer computed by *Fofonoff and Dobson* [1963] (4.5 Sv) and supposed that the upwelling would be two thirds as large at $z = 200$ m, i.e, 3 Sv. This was broadly consistent with his assumption that $\alpha \sim 1/3$.

[30] In our case, estimating $w_E = -\frac{1}{\rho_0}\hat{k} \cdot \nabla \times (\vec{\tau}/f)$ yields a total upwelling of 4.74 Sv at the base of the Ekman layer. Assuming that α is the same over the whole box (0.53) implies 2.23 Sv. This might not be true. Instead, if we integrate the Sverdrup balance from $-h$ (200 m) to 0,

$$w_E - w(-h) = \frac{\beta}{f} \int_{-h}^{0} v_G \, dz. \qquad (8)$$

Summed over the nNP box, the right-hand side equals 1 Sv, thus $V_u \simeq 3.74$ Sv. By consistency with the meridional transport, we consider an error bar of 30% (1.12 Sv).

2.4. Eddy Salt Fluxes

[31] The meridional eddy flux, $\overline{V'S'}$, has been estimated from satellite altimetry by *Stammer* [1998]. His Figure 8b suggests that it is about 10×10^6 kg s^{-1} at 43°N for the upper 1000 m. As we seek its value over the top 200 m, the transport per unit depth it must be multiplied by a factor of 2 or 3 in order to account for surface intensification of the geostrophic flow (D. Stammer, personal communication, 2002); hence $\overline{V'S'} \sim [4–6] \times 10^6$ kg s^{-1}. These numbers are subject to considerable uncertainty.

Table 2. Annual Mean Wind-Stress and Associated Ekman Transports at 43°N

Data Set	Resolution	Mean τ_x[a]	V_E[b]
ASMD	1° × 1°	0.06	4.32
H and R[c]	2° × 2°	0.08	5.88
NCEP/NCAR	2.5° × 2.5°	0.07	5.16
TRENBERTH[d]	2.5° × 2.5°	0.1	6.96

[a]Zonal wind stress (kg m^{-1} s^{-2}).
[b]Meridional Ekman Transport across 43degN (Sv).
[c]Hellerman and Rosenstein Global Wind Stress Data [*Hellerman and Rosenstein*, 1983].
[d]Trenberth global ocean wind stress climatology based on ECMWF analyses [*Trenberth et al.*, 1989].
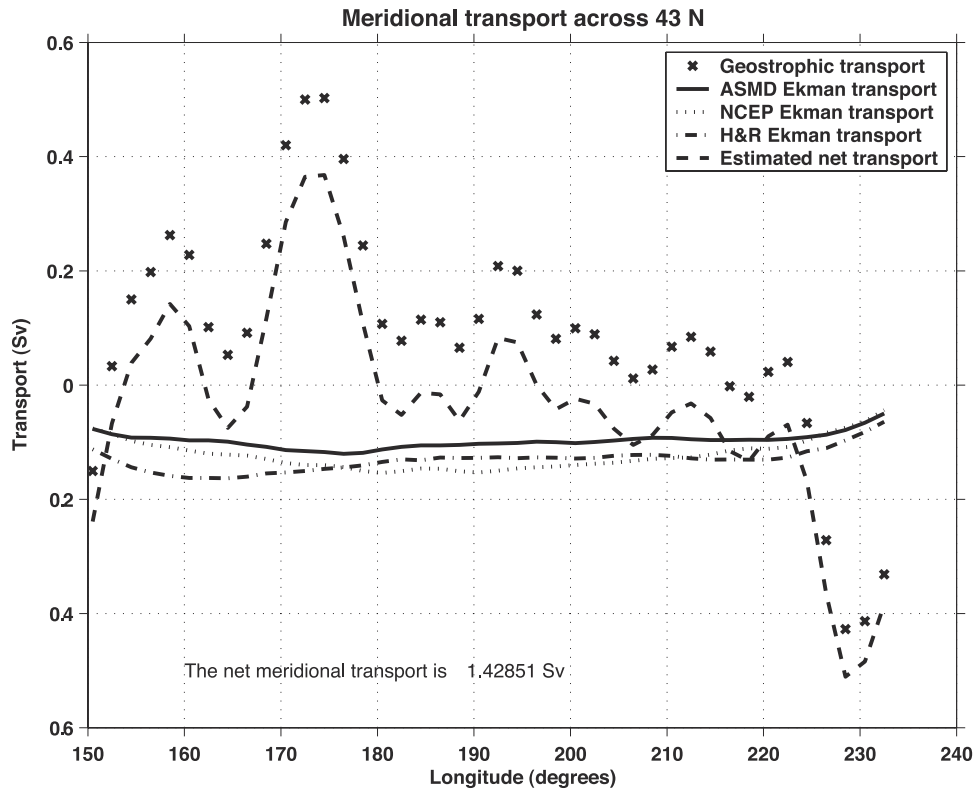
Figure 3. Ekman and geostrophic transports across 43°N, in the top 200 m. The transports are computed east of 150.5°E, with a spacing of 2°. The signature of the California current is very clear east of 140°W.

[32] The vertical eddy flux, $\overline{W'S'}$, may be estimated the same way (equation (4b)), albeit with even greater uncertainty concerning the vertical (approximately diapycnal) eddy diffusivity κ_z (between 10^{-5} and 10^{-4} m^2 s^{-1}). Probably, $\kappa_z \sim [1; 5] \times 10^{-5}$ m^2 s^{-1} is more realistic. Integrating across the area of the basin (deeper than 200 m), this yields $\overline{W'S'} \sim [0.46; 2.3] \times 10^6$ kg s^{-1}.

[33] In Table 3 we summarize the comparison between the boundary fluxes used for the salt budget by BW and this study, together with the uncertainties. Note that BW's estimates all lie within the range of variation of ours, allowed by these error bars. In the row corresponding to BW, V^+ refers to his αV_E, which is equivalent in his formulation. The salinity values of water flowing into the box remained almost the same, i.e., $S_u = 33.7‰$ (the salinity at 200 m) and $S_{WB} = 34‰$. See BW for a discussion.

3. Results

3.1. Basic State and Sensitivity Analysis

[34] In this section we present the results for the nNP box model using the values for fluxes described in the previous section. We first compute the northern North Pacific salinity

for the values presented in Table 3 (the so-called basic state), then we evaluate the sensitivity of the model.

[35] As the functional form of S_s (equations (6) and (7)) depends on the sign of V_{WB}, we first need to estimate the latter. It is determined as a residual from equation (5) using the values for the other quantities given in Table 3. We find that V_{WB} is negative for this range of parameters (about -1.8 Sv), which corresponds qualitatively to the existence of the Oyashio current. Rearranging equation (7), we obtain

$$S_s = \frac{S_u V_u + S_{WB} V^+ + \overline{V'S'} + \overline{W'S'}}{V_u + V^+ + R + F} = \frac{F_s}{V_0}, \quad (9)$$

which is the ratio of a salt flux F_s to the throughflow rate V_0 (more correctly, the "outflow volume transport"). It is noteworthy that the salinity does not depend directly on V_{BS} and V^- in this formulation, but indirectly through mass balance. For the parameters given above, we find $S_s = 32.93‰$, with $V_0 = 4.8 \times 10^9$ kg s^{-1} and $F_s \simeq 160 \times 10^6$ kg s^{-1}, which we will call the reference state. How sensitive is this result to observational and computational errors?

Table 3. Boundary Water Fluxes for the nNP Box (Sv)

	V_{BS}	R	F	V^+	V_u	$\overline{V'S'}$[a]	$\overline{V'S'}$[a]
Warren (1983)	0.8	0.056	0.095	1.485	3	-	-
This study	0.83 ± 0.25	0.03 ± 0.003	0.27 ± 0.15	2.02 ± 0.6	3.74 ± 1.12	5 ± 2	0.46 ± 1.8

[a]Fluxes in 10^6 kg s^{-1}.

Table 4. Sensitivity Terms in the nNP Salt Budget

ζ	F	R	V_u	V^+	$\overline{V'S'}$	$\overline{W'S'}$	S_u	S_{WB}
$\delta\zeta$	0.15	0.003	1.12	0.6	2	1.8	0.1	0.2
$\Delta\zeta$	$-\dfrac{F_s}{V_0^2}\delta F$	$-\dfrac{F_s}{V_0^2}\delta R$	$\dfrac{S_u V_0 - F_s}{V_0^2}\delta V_u$	$\dfrac{S_{WB}V_0 - F_s}{V_0^2}\delta V^+$	$\dfrac{\delta\overline{V'S'}}{V_0}$	$\dfrac{\delta\overline{W'S'}}{V_0}$	$\dfrac{V_u}{V_0}\delta S_u$	$\dfrac{V^+}{V_0}\delta S_{WB}$
$\Delta\zeta$	-0.82	-0.1	0.12	0.14	0.33	0.30	0.06	0.08

[36] To first order, variations in S_s around the reference state are related to those of the parameters ζ_i, $i \in [1; 8]$ by

$$\Delta S_s \simeq \sum_i \frac{\partial S_s}{\partial \zeta_i}\delta\zeta_i \equiv \sum_i \Delta_{\zeta_i}. \qquad (10)$$

The analytical expression of these derivatives, and their value for the error bars ($\delta\zeta_i$) given above are presented in Table 4. Note that for all terms, the second derivatives are of order $1/V_0^2$ for terms with a small $\delta\zeta$ or $1/V_0^4$ for those with a large $\delta\zeta$, and are null for the variables of the last four columns; hence the first order captures the essential part of the variations.

[37] It is obvious that the large error in the freshwater fluxes prevents any determination of S_s with an accuracy better than 0.8‰. We find that this result is rather independent of the reference state used for the linearization. Thus our estimate of 32.93‰ is as close to the observed S_s (33.07) as one can hope. The form of the derivatives suggests that the model is more sensitive to changes in the parameters, particularly the freshwater fluxes, at low throughflow rates V_0 (i.e., for a longer residence time in the box). We note that the second biggest source of uncertainty is the eddy salt transport (about 0.3‰), confirming that mesoscale mixing can affect large-scale quantities to first order, but this does not alter our main result. Nevertheless, it does call for improved estimates of mixing in the ocean.

[38] With the same model, BW came to the conclusion that "the large freshwater flux and the small through-flow rate seem equally important in reducing the surface salinity by so great an amount that no convection can occur. The relatively low salinity of midlatitude surface water entering the region (i.e., the general freshness of the North Pacific in comparison with other oceans) influences somewhat the freshness of the surface water farther north, but that contribution alone is far from sufficient to prevent deep-water formation." Our findings are entirely consistent with these views. We shall now compare this situation to the northern North Atlantic.

3.2. Comparison With the Atlantic

[39] The North Atlantic is roughly 2‰ saltier at the same latitude of 43°N (i.e., $S_{WB} \sim 36$‰), and P-E is much smaller there (Table 1). How would the model respond to such a situation? With $S_{WB} = 36$‰, the model produces $S_s = 33.45$ for the nNP, which is only a modest increase over our basic state. This is a direct consequence of the weak cross-gyre salt transport: For a geostrophic flow and Ekman transport akin to the nNA (scaled by the width of the Pacific), and consistent upwelling, an Atlantic-like $S_{WB} = 36$‰, the model gives $S_s = 34.33$. For an Atlantic-like value of $F = 0.05$ (compare Table 1), the salinity is raised to 34.34‰. With allowance for temporal and spatial variations of 0.3‰

BW, this value is close enough to the deep salinity (34.7‰) to permit wintertime deep convection in some areas of the nNP. We remark that this value of F is well below the lowest estimates of its value over the nNP (Table 1). A less extreme difference is present with other composite difference, for example the 0.17 Sv of the CMAP-ASMD, in which case S_s is only about 33.6‰. Yet the northern North Atlantic has other particularities: The eddy salt transport is about 5 times larger there at 43°N [*Stammer*, 1998], and the cross-gyre flow is much greater. Although the existing density structure may contribute by feeding turbulent eddy mixing through baroclinic instability, and by determining the meridional overturning circulation bringing salty water north, the main part of this cross-gyre flow is wind-driven. The atmospheric flow, through the wind-stress curl pattern, may therefore largely contribute to the ocean salt transport into the nNA, whereas the more zonal wind-stress pattern seems to prevent it in the nNP.

[40] From several independent data sets and reanalyses (Table 1), it is clear that the freshwater flux difference is almost entirely due to the precipitation field ($\sim$0.40 Sv in the nNP, $\sim$0.30 Sv in the nNA). In contrast, the integrated evaporation is strikingly similar in the two basins (about 0.20 Sv). In order to explore the cause of these differences, we use the NCEP Reanalyses [*Kalnay et al.*, 1996], for it also contains information about the moisture and wind field. We remember, however, that their freshwater balance is not entirely consistent with the other data sets, but we make the assumption that the difference between the Atlantic and the Pacific is qualitatively correct.

[41] In Figure 4 we plot the total P-E, E and P fields over the nNP (thick solid line), the nNA (dash-dotted line) and the difference (thin solid line). The difference noted earlier (i.e., that the evaporation is almost identical in the two regions, while the precipitation is about 0.2 Sv greater in the Pacific) seems to hold in all seasons in the Reanalyses. This results in a P-E difference (Pacific - Atlantic) between 0.12 and 0.19 Sv, peaking in May. However, this comparison is biased by the much larger area of the nNP (11.6 versus 6.7×10^{12} m^2). In fact, the values per unit area look quite different: In the nNP, $P = 3.47 \times 10^{-5}$ kg m^{-2} s^{-1}, $E = 1.70 \times 10^{-5}$ kg m^{-2} s^{-1}. In the nNA, the precipitation per unit area is almost as high ($P = 3.28 \times 10^{-5}$ kg m^{-2} s^{-1}), and the evaporation is 1.6 times greater ($E = 2.75 \times 10^{-5}$ kg m^{-2} s^{-1}).

[42] Hence BW's conclusion remains apparently unchanged: As the nNP is rather isolated from southerly oceanic influences, it is the local excess of precipitation over evaporation that makes it so fresh. However, should we be surprised by the fact that the precipitation is relatively high over an ocean that evaporates a lot, or rather, by the high precipitation of the nNP compared to its low evaporation? The real issue is how the evaporative moisture
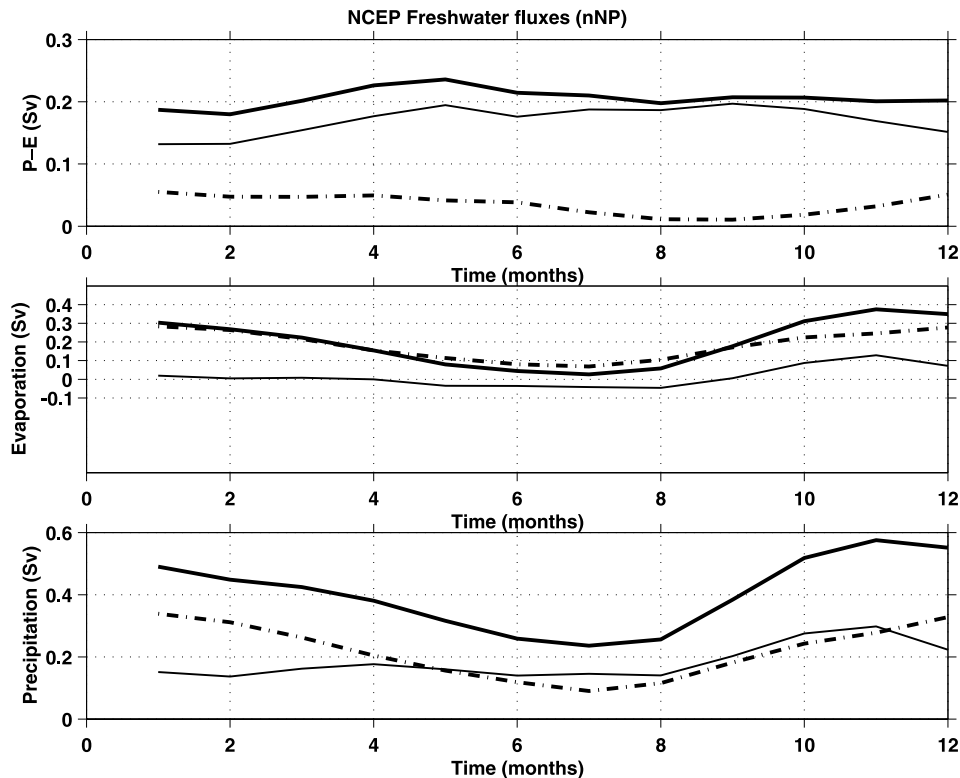
Figure 4. Freshwater fluxes in the NCEP Reanalyses. Thick solid line: nNP; dash-dotted line: nNA; thin line: difference (nNP-nNA).

source is locally balanced: In the absence of atmospheric moisture transports, we would expect *P-E* to vanish over each region. In fact, it nearly does over the nNA (at least in the Reanalyses), but there is a large excess over the nNP. Thus the question "Why is no deep water formed in the North Pacific" becomes "Why is the North Pacific so rainy despite its low evaporation?"

4. Discussion

[43] The reanalysis of the box model developed by BW shows that the local excess of precipitation over evaporation largely sets the stability of the water column, and therefore the absence of deep convection, in the subarctic gyre of the North Pacific. However, one must acknowledge the shortcomings of this model. Intermediate waters (NPIW) are thought to be formed in winter in the Sea of Okhotsk and in the Gulf of Alaska [*You et al.*, 2000], and to be occasionally ventilated in the Alaskan gyre [*Van Scoy and Druffel*, 1993]. NPIW consists of density classes heavier than $\sigma_\theta = 26.7$, which is the mean potential density at 200 m in the nNP. Thus there is some diapycnal mixing with waters below 200 m (the lower boundary of our box), possibly not accounted for by our estimate of vertical eddy mixing. However, the error in ignoring this small flux ought to be negligible compared to other errors in the budget.

[44] The usefulness of this box model lies in its simplicity, and it is only appropriate to investigate the mean equilibrium salinity of the nNP box under a variety of conditions, but we cannot address the timing of the adjustment to varying fluxes, for the steady state assumption led us to ignore seasonal and decadal [*Wong et al.*, 1999] changes in salinity and density. We have also left out any advective feedback, as described by *Rahmstorf* [1995], which makes the model less appropriate for the North Atlantic where this feedback occurs. The model does not take account of deep convection, which is expected to occur in the North Pacific for S_s larger than 34.4 or so. Essentially, the model suggests that under current climatic conditions, it is the low throughflow rate and the large freshwater input over the North Pacific that are responsible for the large-scale relative freshness of the nNP compared to its Atlantic counterpart. Hence we now turn to the source of moisture responsible for the large excess of precipitation over the North Pacific (consistent in the three data sets presented in Table 1). For the western-boundary region, *Roemmich and McCallister* [1989] hypothesize that the moisture excess is due to the monsoon circulation.

[45] In Figure 5 we present the moisture transport, horizontal convergence, and freshwater fluxes for the June–July–August period (JJA) derived from the NCEP Reanalyses. We clearly see the marked difference in the *P-E* term (bottom panel) of the nNA and nNP. The transport is convergent over the whole nNP, and the moisture is carried from the western subtropical Pacific by the large-scale low-level winds associated with the Asian Monsoon, which corroborates the hypothesis of *Roemmich and McCallister* [1989]. No such convergent circulation is found in the Atlantic at the same latitude [*Trenberth et al.*, 2000], which may account for the difference.

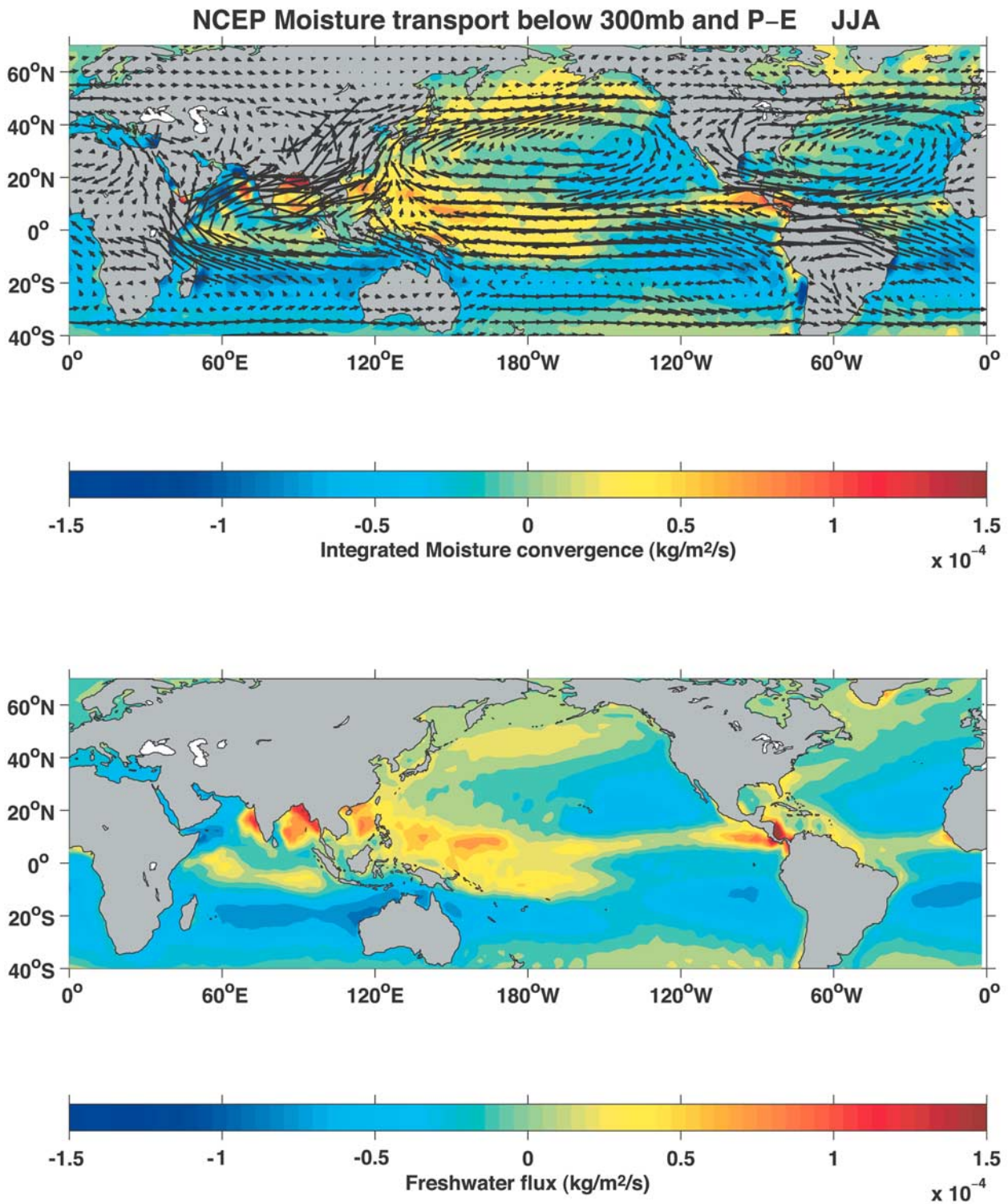[46] The MAM and SON periods are similar, albeit with smaller P-E differences (not shown). However, for the

NCEP Moisture transport below 300mb and P–E   JJA

Integrated Moisture convergence (kg/m²/s)

x 10⁻⁴

Freshwater flux (kg/m²/s)

x 10⁻⁴

Figure 5. Moisture transport, horizontal convergence, and freshwater fluxes for the JJA period (June July August). (top) Moisture transport (arrows) and convergence (contours). (bottom) P-E (contours). The monthly climatology was computed over the period 1949–2002.

winter period (DJF, Figure 6), the interbasin *P-E* contrast is generally strong, albeit weakened along the western boundaries. In this case the outflow of exceedingly dry air from the Asian continent is allowing transfer of moisture from the western boundary current of the subtropical gyre into the subpolar Pacific. Downstream, the moisture is converged rather strongly in the Alaskan gyre, where the *P-E* contrast is greatest. This means of atmospheric freshwater commu-
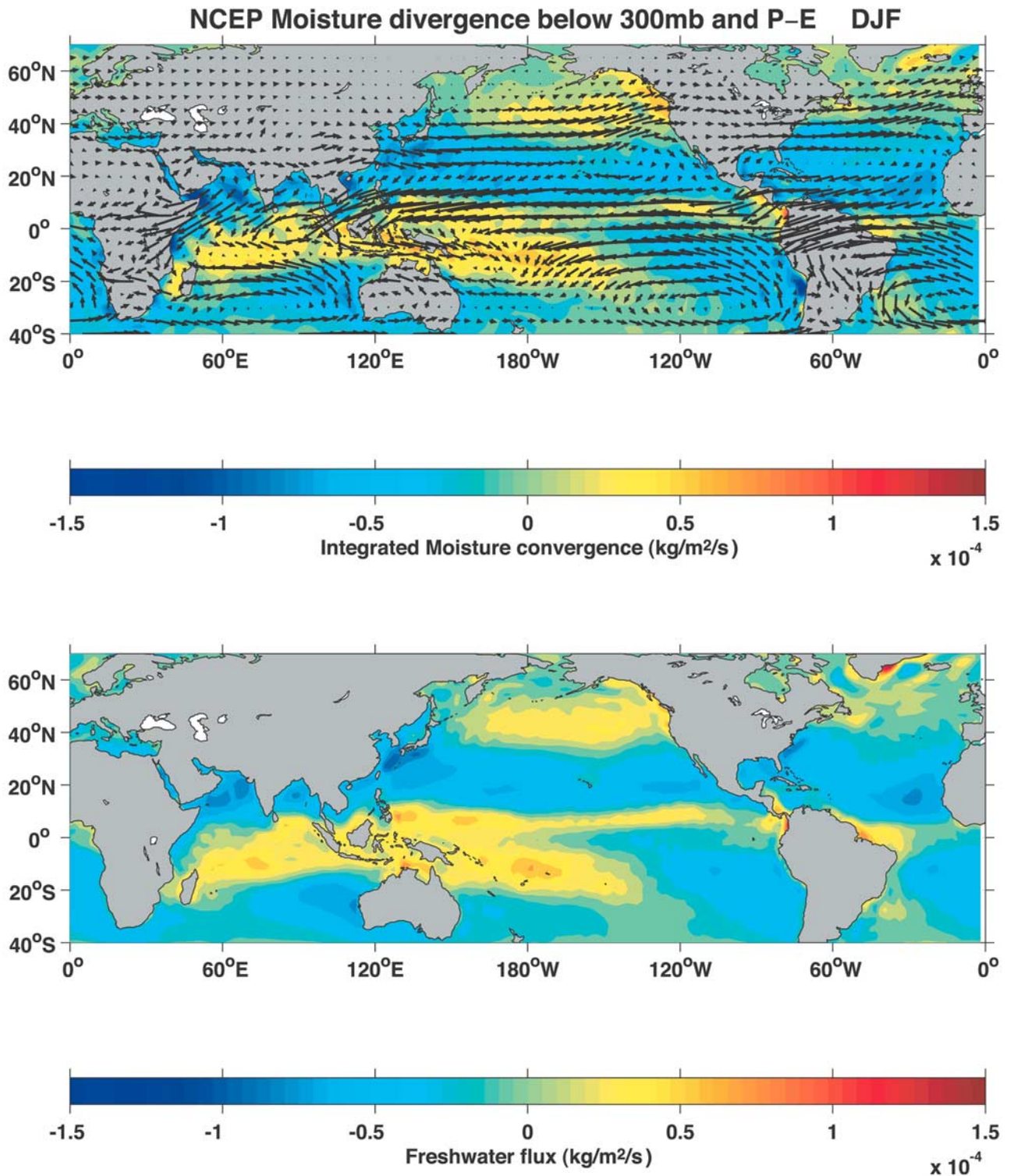
Figure 6. Moisture transport, horizontal convergence, and freshwater fluxes for the DJF period (December January February). (top) Moisture transport (arrows) and convergence (contours). (bottom) P-E (contours). The monthly climatology was computed over the period 1949–2002.

nication between the subtropical and subpolar gyres appears to be stronger in the North Pacific than in the North Atlantic, perhaps because the Atlantic is too narrow for this to happen. This might explain why the total P-E is con-

sistently larger in all season in the nNP (Figure 4): In summer the monsoon circulation transfers important amounts of moisture, presumably originated from the Indonesian seas and the Warm Pool, and converging over the

western nNP; in winter, the circulation picks moisture from the western subtropical gyre and converges it into the northeast North Pacific.

5. Conclusions

[47] We performed an updated analysis of the processes that determine the salinity of the northern North Pacific using the box model described by BW, together with new, more abundant, and presumably more reliable data. We also added estimates of eddy salt transports, unavailable in BW's time. In the light of these firmer, though still imperfect, constraints, we propose that the salinity contrast between the Pacific and the Atlantic subarctic gyres is due to two major factors: (1) The limited oceanic cross-gyre flow and eddy mixing, preventing warm, salty subtropical water from reaching far northern latitudes in the Pacific, and maintaining low evaporation over the nNP. (2) The strength of the Asian monsoon and associated moisture transports. Both factors critically depend on the current land/sea configuration. As emphasized by BW, it is the location of the Himalayas and the Rockies that places the zero-wind-stress-curl line so far south over the North Pacific, thereby isolating the northern North Pacific. The Monsoon itself is the atmospheric response to the seasonal variations in land/sea thermal contrasts.

[48] As a number of conclusions rely on the (questionable) results of the NCEP Reanalyses, the study indicates the need for more complete analysis of global atmospheric freshwater fluxes and their variability, in particular those associated with the Asian Monsoon, and suggest that they might substantially influence the thermohaline circulation asymmetries.

References

Baumgartner, A., and E. Reichel, *The World Water Balance*, R. Oldenbourg Verlag, Munich, Germany, 1975.

Behl, R. J., and J. P. Kennett, Brief interstadial events in the Santa barbara Basin, NE Pacific, during the past 60 kyr, *Nature*, *379*, 243–246, 1996.

Boyle, E. A., Cadmium and δ^{13}C paleochemical ocean distributions during the Stage 2 glacial maximum, *Annu. Rev. Earth Planet. Sci.*, *20*, 245–287, 1992.

Broecker, W. S., The great ocean conveyor, *Oceanography*, *4*, 79–89, 1991.

Broecker, W. S., and G. H. Denton, The role of ocean-atmosphere reorganisations in glacial cycles, *Geochim. Cosmochim. Acta*, *53*, 2465–2501, 1989.

Coachman, L. K., and K. Aagaard, Re-evaluation of water transports in the vicinity of the Bering Strait, in *The Eastern Bering Sea Shelf: Oceanography and Resources*, vol. 1, edited by D. W. Hood and J. A. Calder, pp. 95–110, Natl. Oceanic and Atmos. Admin., Silver Spring, Md., 1981.

Conkright, M., S. Levitus, T. O'Brien, T. Boyer, J. Antonov, and C. Stephens, *World Ocean Atlas 1998 CD-ROM Data Set Documentation*, *Tech. Rep. 15*, 16 pp., Natl. Oceanogr. Data Cent., Silver Spring, MD, 1998.

da Silva, A. M., C. C. Young, and S. Levitus, *Atlas of Surface Marine Data 1994, NOAA Atlas NESDIS 8*, Natl. Oceanic and Atmos. Admin., Silver Spring, Md., 1994.

Dean, W. E., J. V. Gardner, and E. Hemphill-Haley, Changes in redox conditions in deep-sea sediments of the subarctic North Pacific Ocean: Possible evidence for the presence of North Pacific deep water, *Paleoceanography*, *4*, 639–653, 1989.

Fekece, B. M., C. J. Vorosmarty, and W. Grabs, Global, composite runoff fields based on observed river discharge and simulated water balances, technical report, 115 pp., Geol. Res. and Dev. Cent., Bandung, Indonesia, 2000.

Fofonoff, N. P., and F. W. Dobson, Transport computations for the North Pacific Ocean 1950–1959, 10-year means and standard deviations by months; wind stress and vertical velocity, annual means 1955–1960, *Manuscr. Rep. Ser. (Oceanogr. Limnol.) 166*, 179 pp., Fish. Res. Board of Can., Halifax, N.S., Canada, 1963.

Hellerman, S., and M. Rosenstein, Normal monthly wind stress over the world ocean with error estimates, *J. Phys. Oceanogr.*, *13*, 1093–1104, 1983.

Kalnay, E., et al., The NCEP/NCAR Reanalysis Project, *Bull. Am. Meteorol. Soc.*, *77*, 437–471, 1996.

Keigwin, L. D., Glacial-age hydrography of the far northwest Pacific Ocean, *Paleoceanography*, *13*, 323–339, 1998.

Levitus, S., and T. Boyer, *World Ocean Atlas 1994*, vol. 3, *Salinity, NOAA Atlas NESDIS 4*, Natl. Oceanic and Atmos. Admin., Silver Spring, Md., 1994.

Mix, A., D. C. Lund, N. G. Pisias, P. Boden, L. Bornmaln, M. Lyle, and J. Pike, Rapid climate oscillations in the northeast Pacific during the last deglaciation reflect Northern and Southern Hemisphere sources, in *Mechanisms of Global Climate Change, Geophys. Monogr. Ser.*, vol. 112, edited by P. U. Clark, R. S. Webb, and L. D. Keigwin, AGU, Washington, D. C., 1999.

Owens, W. B., and B. A. Warren, Deep circulation in the northwest corner of the Pacific Ocean, *Deep Sea Res., Part I*, *48*, 959–993, 2001.

Rahmstorf, S., Bifurcations of the Atlantic thermohaline circualtion in response to changes in the hydrological cycle, *Nature*, *378*, 145–149, 1995.

Reid, J. L., Jr., Northwest Pacific Ocean waters in winter, *Johns Hopkins Oceanogr. Stud.*, *2*, 85 pp., 1973.

Reid, J. L., Jr., On the total geostrophic circulation of the Pacific Ocean: Flow patterns, tracers, and transports, *Prog. Oceanogr.*, *39*, 263–352, 1997.

Roach, A. T., K. Aagaard, C. H. Pease, S. A. Salo, T. Weingartner, V. Pavlov, and M. Mulakov, Direct measurements of transport and water properties through the Bering Strait, *J. Geophys. Res.*, *100*, 18,443–18,458, 1995.

Roemmich, D., and T. McCallister, Large scale circulation of the North Pacific Ocean, *Prog. Oceanogr.*, *22*, 171–204, 1989.

Stammer, D., On eddy characteristics, eddy transports, and mean flow properties, *J. Phys. Oceanogr.*, *28*, 727–739, 1998.

Sverdrup, H. U., Wind-driven currents in a baroclinic ocean, with application to the equatorial currents of the eastern Pacific, *Proc. Natl. Acad. Sci. U. S. A.*, *33*, 318–326, 1947.

Talley, L. D., Some aspects of ocean heat transport by the shallow, intermediate and deep circulations, in *Mechanisms of Global Climate Change at Millenial Time Scales, Geophys. Monogr. Ser.*, vol. 112, edited by P. U. Clark, R. S. Webb, and L. D. Keigwin, pp. 1–22, AGU, Washington, D. C., 1999.

Trenberth, K. E., and C. J. Guillemot, Evaluation of the atmospheric moisture and hydrological cycle in the NCEP/NCAR reanalyses, *Clim. Dyn.*, *14*, 213–231, 1998.

Trenberth, K., J. Olson, and W. Large, A global ocean wind stress climatology based on ECMWF analyses, *Tech. Rep. NCAR/TN-338 + STR*, Natl. Cent. for Atmos. Res., Boulder, Colo., 1989.

Trenberth, K. E., D. P. Stephaniak, and J. M. Caron, The global monsoon as seen through the divergent atmospheric circulation, *J. Clim.*, *13*, 3969–3993, 2000.

van Geen, A., R. G. Fairbanks, P. Dartnell, M. McGann, J. V. Gardner, and M. Kashgarian, Ventilation changes in the northeast Pacific during the last deglaciation, *Paleoceanography*, *11*, 519–528, 1996.

Van Scoy, K. A., and E. R. M. Druffel, Ventilation and transport of thermohaline and intermediate waters in the Northeast Pacific during recent El Ninos, *J. Geophys. Res.*, *98*, 18,083–18,088, 1993.

Warner, M. J., J. L. Bullister, D. P. Wisegarver, R. H. Gammon, and R. F. Weiss, Basin-wide distributions of chlorofluorocarbons CFC-11 and CFC-12 in the North Pacific: 1985–1989, *J. Geophys. Res.*, *101*, 20,525–20,542, 1996.

Warren, B. A., Why is no deep water formed in the North Pacific?, *J. Mar. Res.*, *41*, 327–347, 1983.

Weyl, P. K., The role of the oceans in climatic change: A theory of the ice ages, *Meteorol. Monogr.*, *8*, 37–62, 1968.

Wijffels, S. E., R. W. Schmitt, H. L. Bryden, and A. Stigebrandt, Transport of freshwater by the oceans, *J. Phys. Oceanogr.*, *22*, 155–162, 1992.

Wong, A. P. S., N. L. Bindoff, and J. A. Church, Large-scale freshening of intermediate waters in the Pacific and Indian Oceans, *Nature*, *400*, 440–443, 1999.

Wyrtki, K., The oxygen minima in relation to ocean circulation, *Deep Sea Res.*, *9*, 11–23, 1962.

Xie, P., and P. A. Arkin, Analysis of global precipitation using gauge observations, satellite estimates and numerical model predictions, *J. Clim.*, *9*, 840–858, 1996.

You, Y., N. Suginohara, M. Fukasawa, I. Yasuda, I. Kaneko, H. Yoritaka, and M. Kawamiya, Roles of the Okhotsk Sea and Gulf of Alaska in forming the North Pacific Intermediate Water, *J. Geophys. Res.*, *105*, 3253–3280, 2000.

Zaucker, F., T. F. Stocker, and W. S. Broecker, Atmospheric freshwater fluxes and their effect on the global thermohaline circulation, *J. Geophys. Res.*, *99*, 12,443–12,457, 1994.

Zheng, Y., A. van Geen, R. F. Anderson, J. V. Gardner, and W. E. Dean, Intensification of the northeast Pacific oxygen-minimum zone during the Bölling-Alleröd warm period, *Paleoceanography*, *15*, 528–536, 2000.

―――――――――――――

M. A. Cane, J. Emile-Geay, N. Naik, R. Seager, and A. van Geen, Lamont-Doherty Earth Observatory, 61 Route 9W, P.O. Box 1000, Palisades, NY 8000-10964, USA. (mcane@ldeo.columbia.edu; julieneg@ldeo.columbia.edu; naomi@ldeo.columbia.edu; seager@ldeo.columbia.edu; avangeen@ldeo.columbia.edu)

A. C. Clement, Rosenstiel School of Marine and Atmospheric Science/MPO, University of Miami, 4600 Rickenbacker Causeway, Miami, FL 33149, USA. (aclement@rsmas.miami.edu)